Preprint Final paper: JMMM Vol. 563, 1 December 2022, 170003 doi 10.1016/j.jmmm.2022.170003

Inkjet-printed Mn-Zn ferrite nanoparticle core for fluxgate

Diana Hrakova[1], Pavel Ripka[1*], Alexander Laposa[1], David Novotny[1], Jiří Kroutil[1], Vojtěch Povolný[1], Ondřej. Kaman[2], Pavel Veverka[2],

[1] *Faculty of Electrical Engineering, Czech Technical University in Prague, 166 27 Prague, Czech Republic*
[2] *Institute of Physics of the Czech Academy of Sciences, 182 00 Prague, Czech Republic*
** corresponding author*

Abstract
Non-planar fluxgate sensors measuring the magnetic fields in the μT range are required for electric current, position, and torque transducers. We report the first sensor based on an inkjet-printed 17 mm diameter ring core. The sensor wide open-loop linear range of ± 1.5 mT allows to operate it without feedback. We describe the preparation of the very stable magnetic ink based on citrate-stabilized 13 nm diameter Mn-Zn ferrite nanoparticles that occur in superparamagnetic regime at room temperature. By printing 100 layers the total thickness of the inkjet-printed core was 2.2 μm. The achieved sensitivity was 10 mV/mT for 25 kHz excitation frequency.

Index Terms—fluxgate, soft magnetic nanoparticles, inkjet printing, flexible magnetic sensor, additive manufacturing

I. INTRODUCTION

Fluxgate is a widely used vectorial magnetic field sensor. Its popularity is based on high sensitivity and low noise level (1 pT to 1 nT/√Hz at 1 Hz) compared to Hall sensors and magnetoresistors [1]. Fluxgates operate at room temperature and have no moving parts. The sensor size ranges from 1 mm (for integrated fluxgates) to 7 cm for precise devices.

The parallel-type fluxgate sensor discussed in this paper is using non-linearity of the sensor ferromagnetic core which is periodically remagnetized by bipolar excitation current. If the measured field is superposed to the excitation, a second harmonic component appears in the output voltage. The core may have a rod, ring, or racetrack shape. Racetrack and rod sensors have higher sensitivity due to the low demagnetization [2]. The excitation of the magnetically open cores is less efficient. Crystalline FeNi permalloy or amorphous cobalt-based alloys are the most popular core materials. Cores of precise fluxgates are made from tapes. Low-cost fluxgates have cores from sputtered or electrodeposited films.

Precise fluxgates are being used for geophysical exploration, monitoring of the Earth's field variations, space research, and for military and security applications such as detection of vehicles or localization of metal objects. Precise fluxgate always utilizes magnetic feedback compensation, which allows achieving ppm linearity [3]. The achievable noise of these devices is 1 pT/√Hz at 1 Hz [4]. Low-cost fluxgates are used in position, torque, and electric current transducers and as a compass in consumer devices. For simple applications, they may operate in the open-loop to save power.

Miniature fluxgates have been manufactured in PCB technology [5-7], glass microfabrication technology [8], CMOS [9, 10], and micromachining [11, 12]. Sensor designs with flat coils such as [13] have a common weak point: the magnetic coupling between the excitation coil and magnetic core is weak, resulting in incomplete saturation of the core and resulting perming error: the offset caused by field shock cannot be erased by excitation field. The only microfluxgate sensor available at the market is Texas Instruments DRV 425 with bar cores and microfabricated solenoid coils [14, 15]. The first flexible fluxgate sensor was developed by Schoinas [16]. The sensor's 40 mm long bar-shaped core is made of amorphous Vitrovac 6025Z tape and the coils are formed by pad printing. The open-loop linear range of this sensor is 40 μT and thanks to the high permeability of the amorphous core it has a high sensitivity of 14 000 V/T. The disadvantage is that the sensor assembly requires manual steps and the sensor properties depend on the tape bending.

In this paper, we describe the first fluxgate with an inkjet-printed core, which allows to fully automatize the core manufacturing process and build the sensor on the substrate of arbitrary shape.

II. SENSOR PRODUCTION

A. Magnetic ink

Mn-Zn ferrite nanoparticles of the composition $Mn_{0.62}Zn_{0.41}Fe_{1.97}O_4$ and the mean size of crystallites (coherent diffraction domain size) of d_{XRD} = 13 nm were prepared under hydrothermal conditions according to the published procedure [17]. The magnetic ink was prepared by stabilizing the particles with ammonium citrate in a mixture of ethylene glycol and water (1:1) as follows. The Mn-Zn ferrite particles were treated with ice-cold 1M HNO_3 in an ultrasound bath for 15 min and were separated by centrifugation. Then the particles were redispersed in ice-cold 0.1 M citric acid in the ultrasound bath for an additional 15 min. The particles were separated by centrifugation, washed with water, and redispersed in water alkalized with a few drops of ammonia by means of a strong ultrasound homogenizer. The raw citrate-stabilized product was subjected to mild size fraction by centrifugation at 116 RCF for 10 min. The supernatant containing the fine fraction was collected, concentrated in vacuo, and mixed with an equal volume of ethylene glycol. The concentration of ferrite particles in the ink was determined to 5.9 mg/ml by SQUID magnetometry of a dried aliquot (taking into account the magnetization of bare particles).

The XRD pattern of the hydrothermally prepared product and a micrograph of the citrate-stabilized particles are shown in Fig. 1. The distribution of hydrodynamic size of particles in the magnetic ink is depicted in Fig. 2 together with the photograph of the ink response to a permanent magnet.

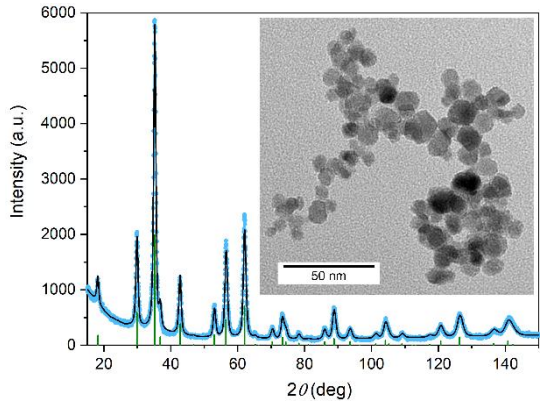

Fig. 1. Powder XRD pattern of $Mn_{0.62}Zn_{0.41}Fe_{1.97}O_4$ ferrite nanoparticles (blue) complemented by the calculated pattern (black) based on the Rietveld refinement. The green markers indicate diffraction lines of the refined spinel structure with the $Fd\bar{3}m$ symmetry and lattice parameter a = 8.4578(2) Å (Bruker D8 Advance diffractometer, Cu Kα radiation). The inset shows a transmission electron micrograph of the particles (Philips CM 120)

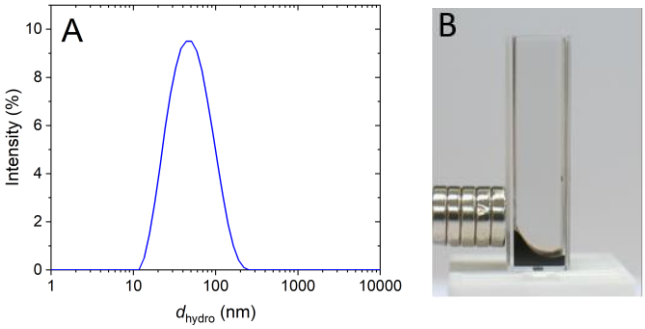

Fig. 2 (a) Intensity distribution of hydrodynamic size of particles in the magnetic ink based on DLS measurement (dynamic light scattering, Malvern Zetasizer Nano ZS) on dilute suspensions in water–ethylene glycol (1:1), Z-average d_z = 42 nm and polydispersity index pdi = 0.233. (b) Visual appearance of the Mn-Zn ferrite ink

B. Printing technology

Printing was carried out by using a drop-on-demand piezoelectric Fujifilm Dimatix DMC-11610 printhead and DMP-2831 inkjet printer with the following conditions: nozzle diameter 21 µm, nominal drop volume of 10 pl, cartridge height 750 µm, ink printing resolution 1016 dpi, print mode 20 times 5 passes (100 layers in total), 1 kHz jetting frequency, drop velocity 8–9 m/s, cartridge temperature 35 °C and substrate temperature 40 °C. Optimal printing conditions were achieved using the theory of Ohnesorge and Weber numbers and optimization of the piezoelectric printhead actuating voltage waveform [21], Fig. 3. PET foil from Mitsubishi Novele™ IJ-220 (thickness of 140 µm) was used as a substrate. The ink has stable printing properties, and no ink degradation was observed when stored at room temperature for several months. The thickness of the inkjet-printed core was 2.2 µm.The sample printed lines and dots are shown in Fig. 4. The final structure was overprinted by a protective coating based on UV curable epoxy-based thermoset ink.

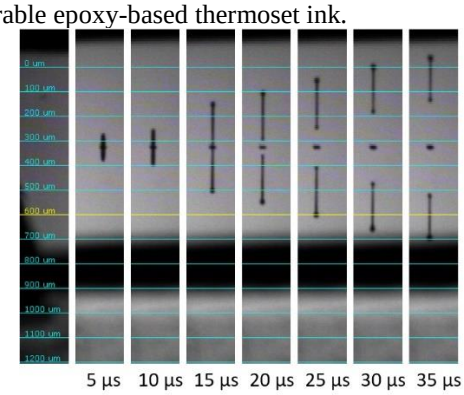

Fig. 3. View of the droplet formation sequence

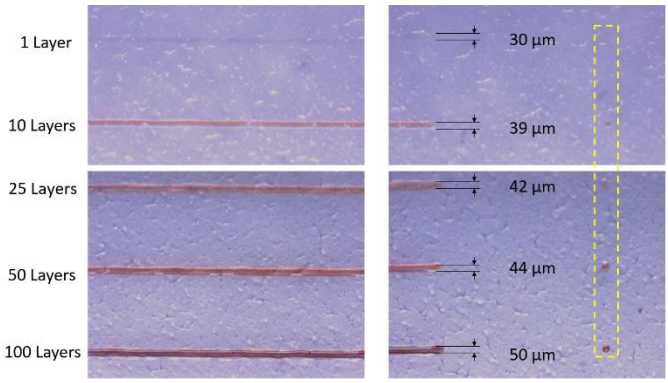

Fig. 4. Printed lines and dots of the Mn-Zn ferrite ink on PET substrate with various number of layers and measured width of the structures

C. Fluxgate sensor production

The ring-shaped printed core of 13/17 mm size has 100 layers (Fig. 5). The core was fixed inside the toroidal 12/18 mm bobbin, which serves for the mechanical protection of the core and support for the excitation winding.

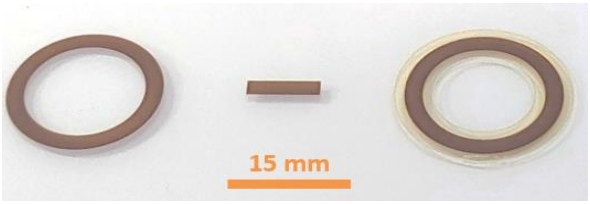

Fig. 5. Ring-shaped inkjet-printed core (left) and inkjet printed UV cured coating (right). The straight bar (middle) is a sample printed for SQUID measurements.

The excitation coil has 110 turns of 0.28 mm diameter copper wire. It has a resistance R_{exc} = 450 mΩ and inductance L_{exc} = 4.5 µH. The wound core was inserted inside the rectangular pick-up coil with 1500 turns of 0.1 mm diameter.

III. SQUID MEASUREMENTS

Rectangular 2 mm * 2 mm samples were cut from the printed film for SQUID measurements. Fig. 7 shows the magnetization

curve for the 100-layers film, which is either anhysteretic or shows a coercivity below the experimental limit (due to remnant fields in the superconducting solenoid). Zero-field-cooled (ZFC) and field-cooled (FC) susceptibility study on the dried magnetic ink is depicted in Fig. 8, including the temperature derivative of the difference between the respective susceptibilities, which gives the distribution of blocking temperatures. The sample is almost entirely in the superparamagnetic regime (on the time scale of ≈10–10^2 s).

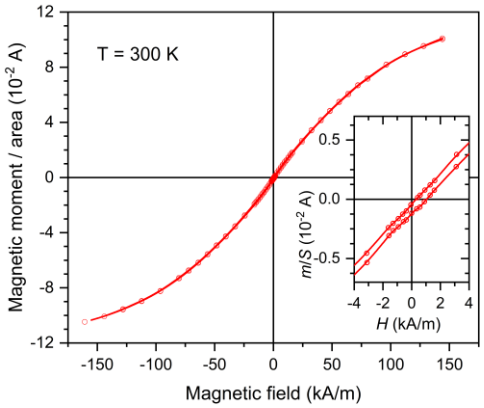

Fig. 6. Hysteresis loop of the inkjet-printed core measured by SQUID

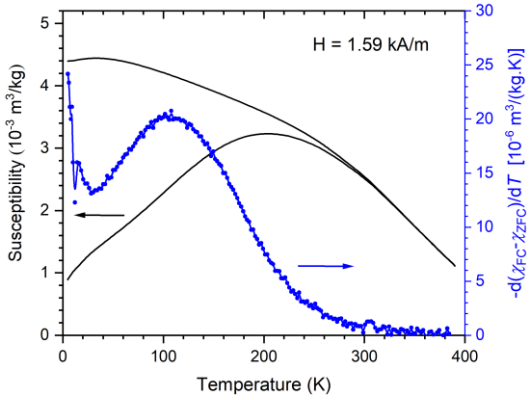

Fig. 7 ZFC-FC susceptibility measurements of the dried ink (temperature derivative of the ZFC-FC susceptibility difference on the right axis)

The crystallographic density of the used nanoparticles is 5.17 g/cm^3. Measuring a pure powder at 300 K in a 3 T field gives a magnetization of 55.0 Am^2/kg, and based on this result it is possible to find a volume magnetization of 284.4 x 10^3 A/m, which after multiplying μ_0 gives 0.357 T.

The magnetic nanoparticles of this type cannot be fully saturated even in a large field. The linear paramagnetic process of ferrite nanoparticles is related to the disruption of the ferromagnetic arrangement in the surface layer, where the atomic spins are essentially disordered and show a paramagnetic response. This layer is about 2 nm thick and is volumetrically significant for nanoparticles.

IV. SENSOR CHARACTERISATION

A. The sensor excitation

In order to achieve a low perming effect and high offset stability, the fluxgate sensor should be deeply saturated by the excitation current. For conventional fluxgate sensors, this is achieved by nonlinear excitation tuning by a parallel capacitor, which results in excitation current with high narrow peaks; thus the core is saturated without overheating of the excitation coil [18]. However, this is not possible for small cores or cores with low permeability, giving a low-quality factor of the excitation coil. The solution to this problem is to use a pulse-shaped excitation current [19]. 100 ns pulses are used in DRV 425 integrated fluxgate excitation [20].

Our sensor is excited by the custom-made pulse generator with the power stage based on the H-bridge. Serial resistor R_s = 3.33 Ω was used to decrease the time constant of the excitation circuit to L_{exc} / (R_{exc} + R_s), where L_{exc} and R_{exc} are the inductance and resistance of the excitation coil respectively. During the off-state, the excitation coil is short-circuited into the same resistor. We also used a large serial capacitor to decouple any DC component of the excitation current, which would cause sensor offset (through the unavoidable sensor asymmetry). The measurements of the sensitivity were done at frequencies 10–200 kHz with a duty cycle of 10 – 20%. The fluxgate effect for this core excited at mentioned frequencies is observed for excitation voltage V_{exc} > 2.6 V. We measured the sensor characteristics for V_{exc} = 5 V and 10 V.

B. The testing setup

The sensor characteristics were measured in the Helmholtz coils supplied by DC power source Toellner TOE 8871 in the field range of ± 6.5 mT. The testing setup is shown in Fig 8.

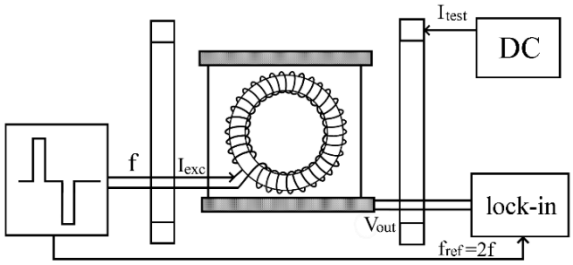

Fig. 8. Measurement setup.

The 2nd harmonic component of the output voltage was measured by the SR865 DSP lock-in amplifier.

The important signal waveforms are shown in Fig 9. Despite the low permeability of the used core, the inductance of the excitation coil was much higher than that of integrated fluxgates. This is the reason for the much slower increase of the excitation current.

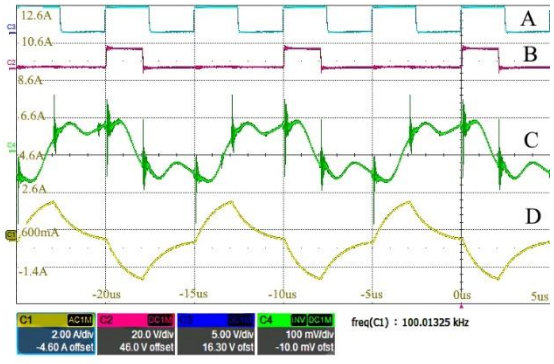

Fig. 9. Measured waveforms for f_{exc} = 100 kHz, V_{exc} = 10 V, duty = 20 %: (a) 2nd harmonic reference, (b) positive excitation control pulses, (c) output voltage for B = 0, (d) excitation current

C. The measured results

Fig. 10 shows the sensor output 2nd harmonic voltage as a function of the measured field in an open-loop for several parameters of the excitation. The sensitivity is increasing with the excitation amplitude, indicating that the sensor excitation amplitude is below the optimum value. The transfer curve is linear within ± 1.5 mT, which is an unusually high range for open-loop operation: the published values are between 40 μT [13] and 500 μT.

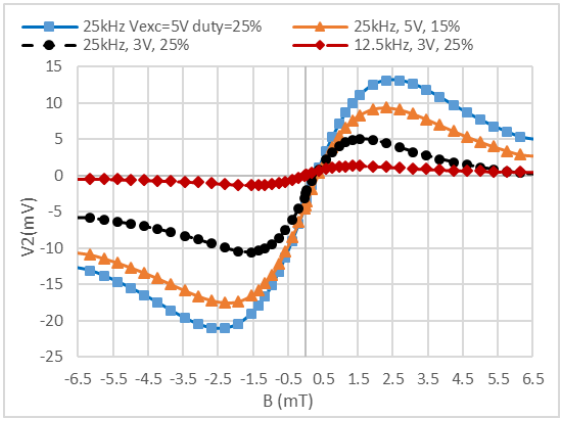

Fig. 10. Fluxgate transfer characteristics

V. CONCLUSION

We report the first fluxgate sensor with an inkjet-printed core based on nanoparticles. Both excitation and pickup coils were conventionally wound by copper wire; in the future, we plan to make these windings with 3D printing technology. The main advantage of the sensor is its very wide open-loop linear range of ± 2 mT. The current disadvantage is low sensitivity of 10 mV/mT, which we plan to improve by optimization of the core magnetic properties and excitation parameters. One possible way of increasing core permeability is applying a static magnetic field while ink jetting the particles [22].The target application of the printed fluxgate sensors is not a precise measurement of the magnetic field, but electric current, position, and torque transducers, which will benefit from the sensors printed on non-planar surfaces. Another possible application field is position sensing for wearable devices.

ACKNOWLEDGMENT

This study was supported by the Grant Agency of the Czech Republic within the Nanofluxgate project (GACR GA20-27150S). SQUID measurements carried out in MGML (mgml.eu), supported within the Czech Research Infrastructures (project no. LM2018096).

REFERENCES

[1] P. Ripka, *Magnetic sensors and magnetometers, 2nd edition*, Boston, London: Artech House, 2021.

[2] J. Kubík, and P. Ripka, "Racetrack fluxgate sensor core demagnetization factor," *Sens. Actuator A Phys.*, vol. 143, no. 2, pp. 237-244, May 2008.

[3] D. Novotny, and V. Petrucha, "High Dynamic Range Digital Fluxgate Magnetometer," *IEEE Sensors conf.* 2020, doi: 10.1109/SENSORS47125.2020.9278852.

[4] M. Janosek, M. Butta, M. Dressler *et al.*, "1-pT Noise Fluxgate Magnetometer for Geomagnetic Measurements and Unshielded Magnetocardiography," *IEEE Trans. Instrum. Meas.*, vol. 69, no. 5, pp. 2552-2560, May 2020.

[5] O. Dezuari, E. Belloy, S. E. Gilbert *et al.*, "Printed circuit board integrated fluxgate sensor," *Sens. Actuator A Phys.*, vol. 81, pp. 200-203, Apr. 2000.

[6] P. Kejik, L. Chiesi, B. Janossy *et al.*, "A new compact 2D planar fluxgate sensor with amorphous metal core," *Sens. Actuator A Phys.*, vol. 81, no. 1-3, pp. 180-183, Apr. 2000.

[7] J. Kubik, L. Pavel, and P. Ripka, "PCB racetrack fluxgate sensor with improved temperature stability," *Sens. Actuator A Phys.*, vol. 130-131, pp. 184-188, 2006.

[8] T. Heimfarth, M. Z. Mielli, M. N. P. Carreno *et al.*, "Miniature Planar Fluxgate Magnetic Sensors Using a Single Layer of Coils," *IEEE Sens. J.*, vol. 15, no. 4, pp. 2365-2369, Apr. 2015.

[9] S. Kawahito, H. Satoh, M. Sutoh *et al.*, "High-resolution micro-fluxgate sensing elements using closely coupled coil structures," *Sens. Actuator A Phys.*, vol. 54, no. 1-3, pp. 612-617, Jun. 1996.

[10] L. Chiesi, P. Kejik, B. Janossy *et al.*, "CMOS planar 2D micro-fluxgate sensor," *Sens. Actuator A Phys.*, vol. 82, no. 1-3, pp. 174-180, May 2000.

[11] T. M. Liakopoulos, and C. H. Ahn, "A micro-fluxgate magnetic sensor using micromachined planar solenoid coils," *Sens. Actuator A Phys.*, vol. 77, no. 1, pp. 66-72, Sep. 1999.

[12] C. Lei, X. C. Sun, and Y. Zhou, "Noise analysis and improvement of a micro-electro-mechanical-systems fluxgate sensor," *Measurement*, vol. 122, pp. 1-5, Jul. 2018.

[13] P. H. Hsieh, and S. J. Chen, "Multilayered vectorial fluxgate magnetometer based on PCB technology and dispensing process," *Meas. Sci. Technol.*, vol. 30, no. 12, Dec. 2019.

[14] M. F. Snoeij, V. Schaffer, S. Udayashankar *et al.*, "Integrated Fluxgate Magnetometer for Use in Isolated Current Sensing," *IEEE J. Solid-State Circ.*, vol. 51, no. 7, pp. 1684-1694, Jul. 2016.

[15] V. Petrucha, and D. Novotny, "Testing and application of an integrated fluxgate sensor DRV425," *J. Electr. Eng. - Elektrotechnicky Casopis*, vol. 69, no. 6, pp. 418-421, Dec. 2018.

[16] S. Schoinas, A. M. El Guamra, F. Moreillon *et al.*, "Fabrication and Characterization of a Flexible Fluxgate Sensor with Pad-Printed Solenoid Coils," *Sensors*, vol. 20, no. 8, art. no. 2275, Apr. 2020.

[17] O. Kaman, D. Kubaniova, K. Knizek *et al.*, "Structure and magnetic state of hydrothermally prepared Mn-Zn ferrite nanoparticles," *J. All. Comp.* vol. 888, art. no. 161471, Dec. 2021.

[18] P. Ripka, and W. G. Hurley, "Excitation efficiency of fluxgate sensors," *Sens. Actuator A Phys.*, vol. 129, no. 1-2, pp. 75-79, May 2006.

[19] P. Ripka, S. O. Choi, A. Tipek *et al.*, "Pulse excitation of micro-fluxgate sensors," *IEEE Trans. Magn.* vol. 37, no. 4, pp. 1998-2000, Jul. 2001.

[20] M. F. Snoeij, V. Schaffer, S. Udayashankar *et al.*, "An Integrated Fluxgate Magnetometer for use in Closed-Loop/Open-Loop Isolated Current Sensing," Proc. ESSCIRC Conf. 2015

[21] B. Derby, "Inkjet printing of functional and structural materials: Fluid property requirements, feature stability, and resolution," *Annu. Rev. Mater. Res.*, vol. 40, no. 1, pp. 395–414, Jun. 2010.

[22] K. N. Al-Milaji, R. L. Hadimani, S. Gupta *et al.*, "Inkjet Printing of Magnetic Particles Toward Anisotropic Magnetic Properties," *Scientific Reports*, vol. 9, no. 1, Dec. 2019